

AD-A122 083

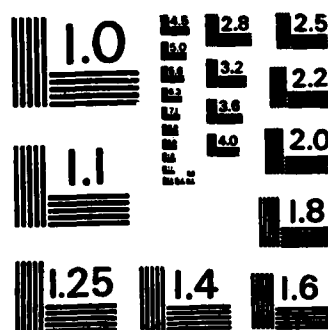
STRENGTH OF LUMBER UNDER COMBINED BENDING AND
COMPRESSION(U) FOREST PRODUCTS LAB MADISON WI J J ZAHN
SEP 82 FSRP-FPL-391

1/1

UNCLASSIFIED

F/G 11/12 NL





MICROCOPY RESOLUTION TEST CHART
 NATIONAL BUREAU OF STANDARDS-1963-A

AD A 122083

United States
Department
of Agriculture

Forest Service

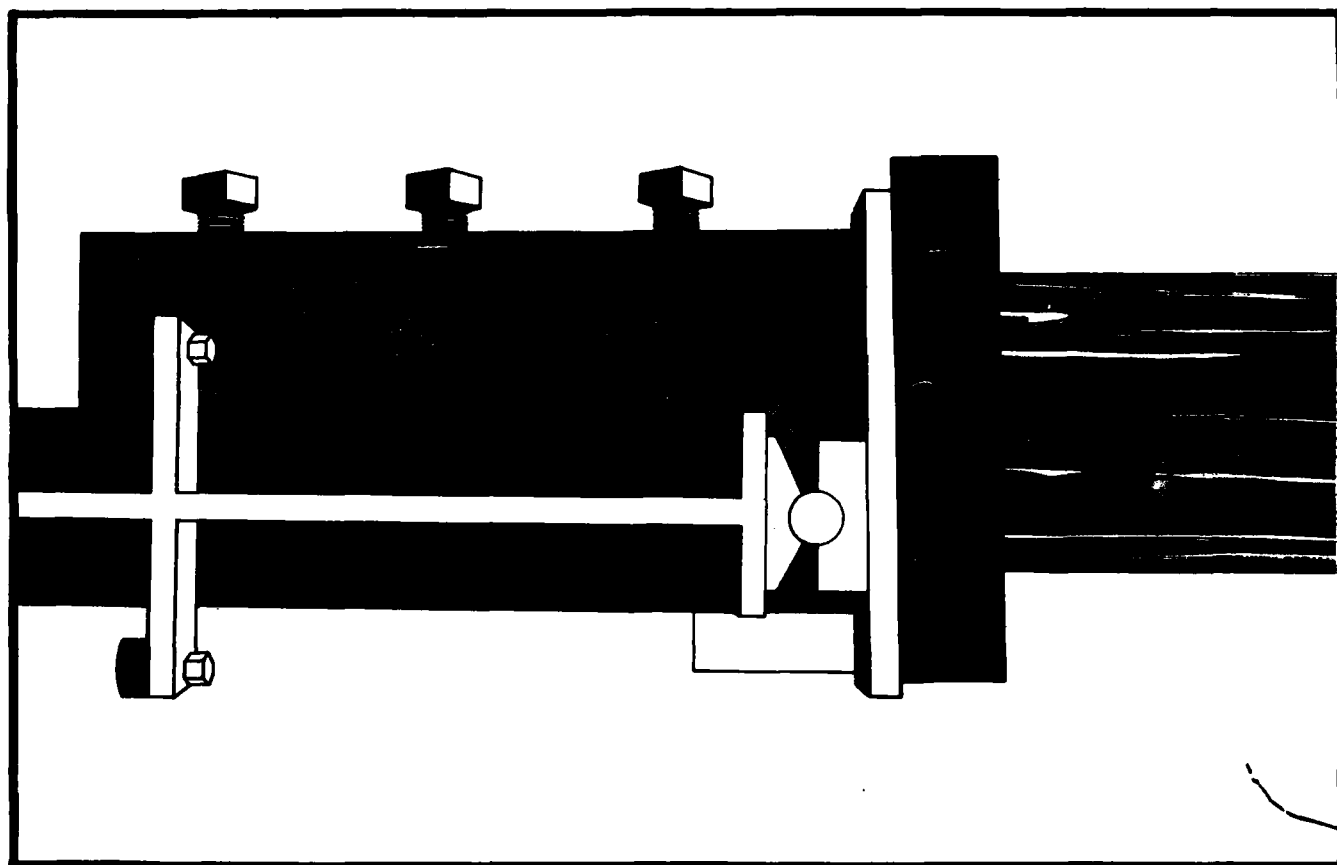
Forest
Products
Laboratory

Research
Paper
FPL 391



Strength of Lumber Under Combined Bending and Compression

12



DTIC FILE COPY

This document has been approved
for public release and sale; its
distribution is unlimited.

DTIC
ELECTE
DEC 0 6 1982
S D E

82 12 06 061

Abstract

It is conjectured that the addition of a small compressive force might increase bending strength. Extensive tests of western hemlock 2 by 6's under eccentric axial load bear this out. Test members were short but length effect is studied analytically by simulating long members with a finite element computer program. A small sample of long members was tested to verify the computer model. Verification was not thorough but the model appears to do very well. It accurately reproduces the mean but underestimates the variance. Further work on the model is planned. This work will have important applications to column design and wood truss design.

Acknowledgment

This work was begun while the author was stationed in Vancouver, British Columbia at the Western Forest Products Laboratory (subsequently re-organized as part of FORINTEK Canada) on a 1-year visit as part of a scientist exchange between Forest Products Laboratory in Madison and the WFPL. All materials were purchased by the WFPL and all tests were performed with their equipment and technicians. Computer tapes of raw data were brought back to the United States where data analysis was performed and this report written. The author wishes to express his gratitude to his Canadian hosts for their gracious hospitality and especially recognizes Dr. Robert Sexsmith for his many helpful discussions.

United States
Department of
Agriculture

Forest Service

Forest
Products
Laboratory¹

Research
Paper
FPL 391

September 1982

Strength of Lumber Under Combined Bending and Compression

By
JOHN J. ZAHN, Research General Engineer

Accession For	
NTIS GRA&I	<input checked="" type="checkbox"/>
DTIC TAB	<input type="checkbox"/>
Unannounced	<input type="checkbox"/>
Justification	
By	
Distribution/	
Availability Codes	
Dist	Avail and/or Special
A	

Introduction

Wood members under combined bending and compression occur as structural elements in several important applications: as the top chords of trusses, as wall studs, as frame members in towers, and in other rigid frame structures. While strength in bending alone and compression alone have been extensively studied, the interaction of these two modes of failure is poorly understood, particularly for dimension lumber of common construction grades. There is reason to expect that a moderate compressive force acting in concert with a bending moment could raise the moment capacity by shifting the mode of failure from a defect-controlled brittle rupture to a more ductile compression failure (1).² Plastic buckling could become a failure mode. In the absence of good data on failure under combined bending and compression, present design recommendations are quite conservative; this conservatism is a major economic factor in the wood roof truss industry.

Experimental

Design of Experiments

The aim of this study was to define a failure locus in the plane of bending moment (M) versus compressive force (C). Attention was restricted to that portion of the plane where bending stress exceeds compressive stress since that is the region of greatest importance in the design of wood frame structures and trussed roofs.

In order to limit the scope of the study, only one species (Western Hemlock) and one size (nominal 2 x 6) were studied. The effects of length and grade of material were recognized as critical but rather than test several combinations of length and grade it was decided to simulate these effects with a finite-element computer program. In that way only short pieces (single "elements") need be tested to establish a data pool from which a computer program can select elements and mathematically simulate the behavior of longer members. The effect of material grade was incorporated by measuring a quality index for each element. The edgewise bending stiffness was chosen for this index because it is known to have the best correlation with bending strength of any nondestructive measurement. In addition to establishing the data pool of element properties, a few longer members were tested to verify the finite element model's predictive ability.

Thus, the aims of the experimental program were twofold:

1. To test short members under combined bending and compression at various M/C ratios. For this purpose four large groups of specimens were tested, three under eccentric axial load at different eccentricities and one in pure bending.
2. To verify the computer-simulated behavior of longer members. For this (secondary) purpose, a small group of 8-foot long members were quality-rated and then tested under eccentric axial load.

The resulting experimental design is shown in table 1.

Material

Western hemlock of 10-foot and 12-foot lengths was purchased from the Eburn mill of the Canadian Forest Products

¹ Maintained at Madison, Wis., in cooperation with the University of Wisconsin.

² Italicized numbers in parentheses refer to literature cited at end of this report.

Table 1.—Summary of tests performed

Group	Moment	Number of specimens	Gage length	Direction of load
	Axial load			
	in.		in.	
1	1	101	18	Axial eccentric
2	1.5	102	18	Axial eccentric
3	3.5	104	18	Axial eccentric
4	∞	124	18	Lateral
5	1	29	96	Axial eccentric

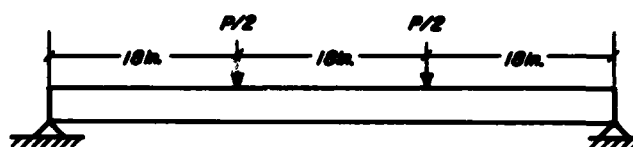
¹ These had been planned to be 125 each, but tests were discarded whenever failure occurred outside the gage length.

Company. An effort was made to select members with a No. 2 grade defect in the gage length portions of two 5-foot members to be cut from each longer length. Since western hemlock and white fir are marketed together, each piece had to be identified by microscopic examination of cell structure and the white fir segregated for use in other studies.

Specimen Preparation

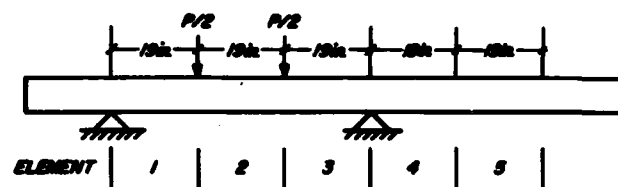
Five-hundred specimens 5 feet long were cut with an effort to position defects in the center 18 inches of the piece whenever possible. Thirty members 11 feet long were cut from pieces deemed not suitable for the short specimens. Short specimens were quality rated by testing in edgewise bending to a load of 300 pounds. Two-point load was applied at the third points as shown in figure 1. An online computer took digitized readings of load and head movement at two points and computed an "E-rating" value, E_T , from the formula

$$E_T = \frac{5(P_2 - P_1)L^3}{27(H_2 - H_1)bh^3}$$



M 140 000

Figure 1.—Loading used for E-rating specimens in groups one to four.



M 140 040

Figure 2.—Loading used for E-rating specimens in group five. The member was rated five times, one for each 19-inch element. The position shown here is for rating element 2.

where P = load, H = head movement, L = 54 inches, b = width, and h = depth. The 11-foot specimens were each quality rated at five different positions by a similar test in edgewise bending under two-point loading as shown in figure 2. Between readings the member was indexed through the test machine in 19-inch increments. Again a computer used head movement and machine load to compute E_T for each of five "elements" in the central 8-foot gage length of these 11-foot members.

Table 2.—Summary of experimental results

Properties	Groups				
	1	2	3	4	5
Ultimate axial load, P_u , lb	31,308 (0.212)	24,800 (0.225)	13,300 (0.296)	¹ —	16,900 (0.349)
Center deflection at ultimate load, Δ_u , in.	1.17 (.069)	1.69 (.038)	3.72 (.022)	¹ —	¹ —
Ultimate moment M_u , in. lb	36,400 (.225)	40,700 (.229)	49,600 (.290)	47,100 (0.426)	¹ —
Quality index E_T , 10 ⁶ lb/in. ²	1.04 (.100)	1.05 (.169)	1.03 (.211)	1.04 (.157)	0.981 (.206)
Apparent modulus $\frac{E_T}{I}$, 10 ⁶ lb/in. ²	2.16 (.277)	1.91 (.254)	1.89 (.290)	2.16 (.247)	—
Specific gravity	0.483 (.122)	0.484 (.105)	.448 (.137)	.452 (.120)	.435 (.131)
Moisture content, pct	11.2 (.009)	11.2 (.057)	11.3 (.054)	12.8 (.091)	10.4 (.040)

¹ Mean value (coefficient of variation).

² Does not apply (Group 4 was tested in bending).

³ Not obtained.

⁴ Includes the eccentricity, i.e., it is measured from the line of action of the axial load.

⁵ E_T was of the center element in Group 5.

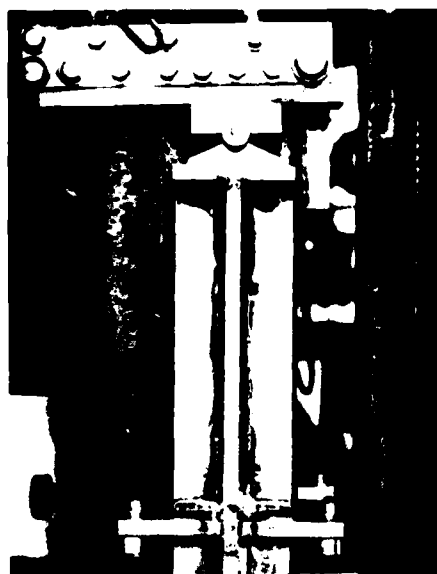
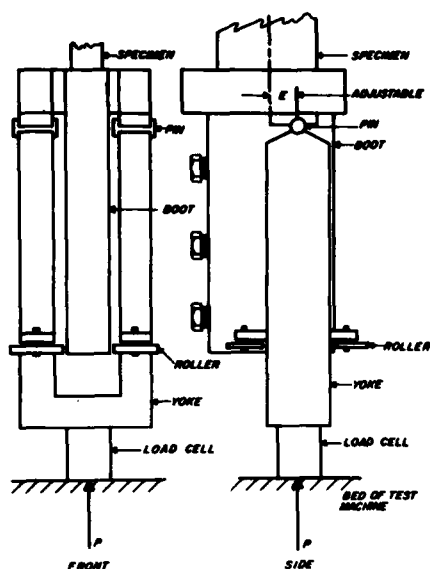


Figure 3.—Loading fixture for applying eccentric axial load: A) diagram, B) photo of side view, and C) photo looking into empty boot. Rope restrains boot from falling out when specimen fails.

The short members were sorted in order of increasing E_r . The first four were randomly assigned to groups 1 through 4. The next four were then randomly assigned, and the next four, etc., until four matched groups were produced with nearly identical distributions of E_r . Table 2 shows how closely the E_r distributions of groups one to four agreed. Means ranged from 1.03 to 1.05 million pounds per square inch and coefficients of variation ranged from 0.157 to 0.211.

Test Methods

Groups One to Three

Eccentric axial load was applied through grips in the form of steel boots 18 inches long. The top of the boot bore against the end of the specimen. The narrow sides of the boot were made snug against the specimen by means of adjusting screws shown in figure 3. The bottom of the boot had flanges which received the test machine load by way of a yoke which straddled the boot. This put the pivot point as close to the gage length as possible in order to minimize the growth of eccentricity due to specimen deformation during a test. Since inservice wall studs and roof truss chords are restrained against lateral buckling by sheathing materials, the test specimens were laterally supported at midspan by fixed braces on each side of the specimen. Initially there was an 1/8-inch clearance between the specimen and the lateral supports and the support braces were surfaced with a hard polished plastic having a low coefficient of friction. In this manner the specimens were constrained to deflect only in the direction of greatest stiffness.

Deformation measurements were taken by two linear variable differential transformers (LVDT's) at the ends of arms attached to the wide faces of the specimen, as shown in figure 4. The arms were clamped to the specimen with an 18-inch gage length between them. The two deflection readings y_1 and y_2 are related to axial deflection and curvature as follows:

$$\Delta l = \frac{1}{2}(y_1 + y_2) \quad (2)$$

$$\frac{1}{R} = \frac{2(y_1 - y_2)}{a(2l + y_1 + y_2)} \quad (3)$$

where Δl = axial elongation (contraction if negative), R = radius of curvature, l = gage length (18 in.), and a = arm length (14 in.).

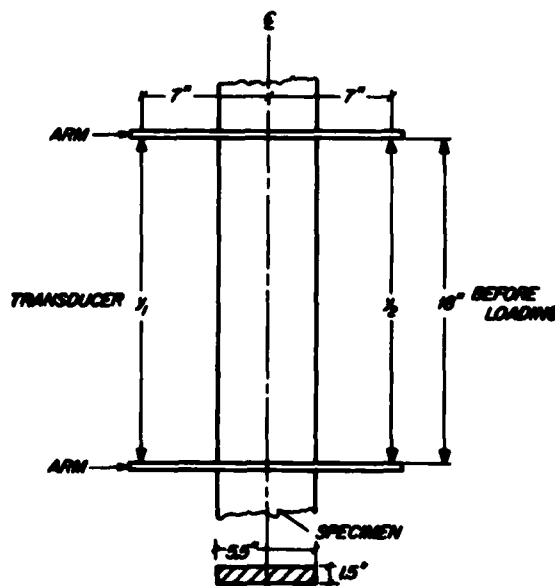


Figure 4.—Deflectometer arrangement. Rigid arms were clamped to specimen and linear variable differential transformers (LVDT's) were mounted between them at 7 inches on either side of center line.

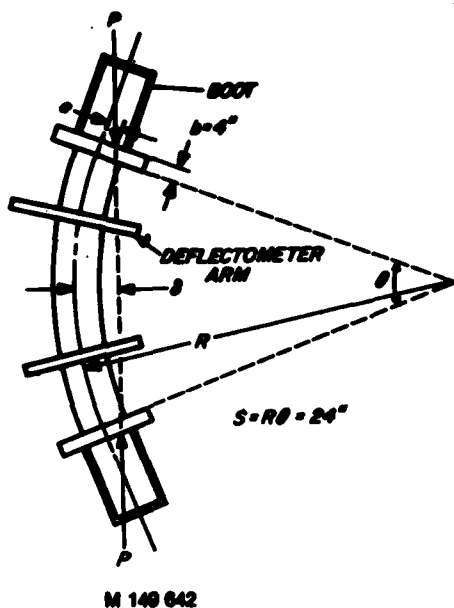


Figure 5.—Exaggerated specimen deformation showing curvature and center deflection, δ

The moment applied to the specimen by the eccentric axial load is

$$M = P\delta \quad (4)$$

where δ equals lateral deflection of specimen centroidal axis measured from line of action of P. During test, the boots rotate through an angle θ

$$\theta \approx \frac{S}{R} \quad (5)$$

where S equals arc length between boots, which is 24 inches (see figure 5). Thus δ can be computed from

$$\delta = e \cos \frac{\theta}{2} + b \sin \frac{\theta}{2} + R(1 - \cos \frac{\theta}{2}) \quad (6)$$

where e = eccentricity and $b = 4$ inches = distance from pivot point to edge of boot.

Data Recording

Load P and deflections y_1 and y_2 were recorded automatically on punched paper tape with the aid of an online computer and teletype machine (see figure 6). An X-Y plotter recorded y_1 and y_2 versus P. The paper tapes were later read by another computer and reduced to R, P, and δ and stored on magnetic tape. These magnetic tapes and the X-Y plots form a permanent record of the raw test data.

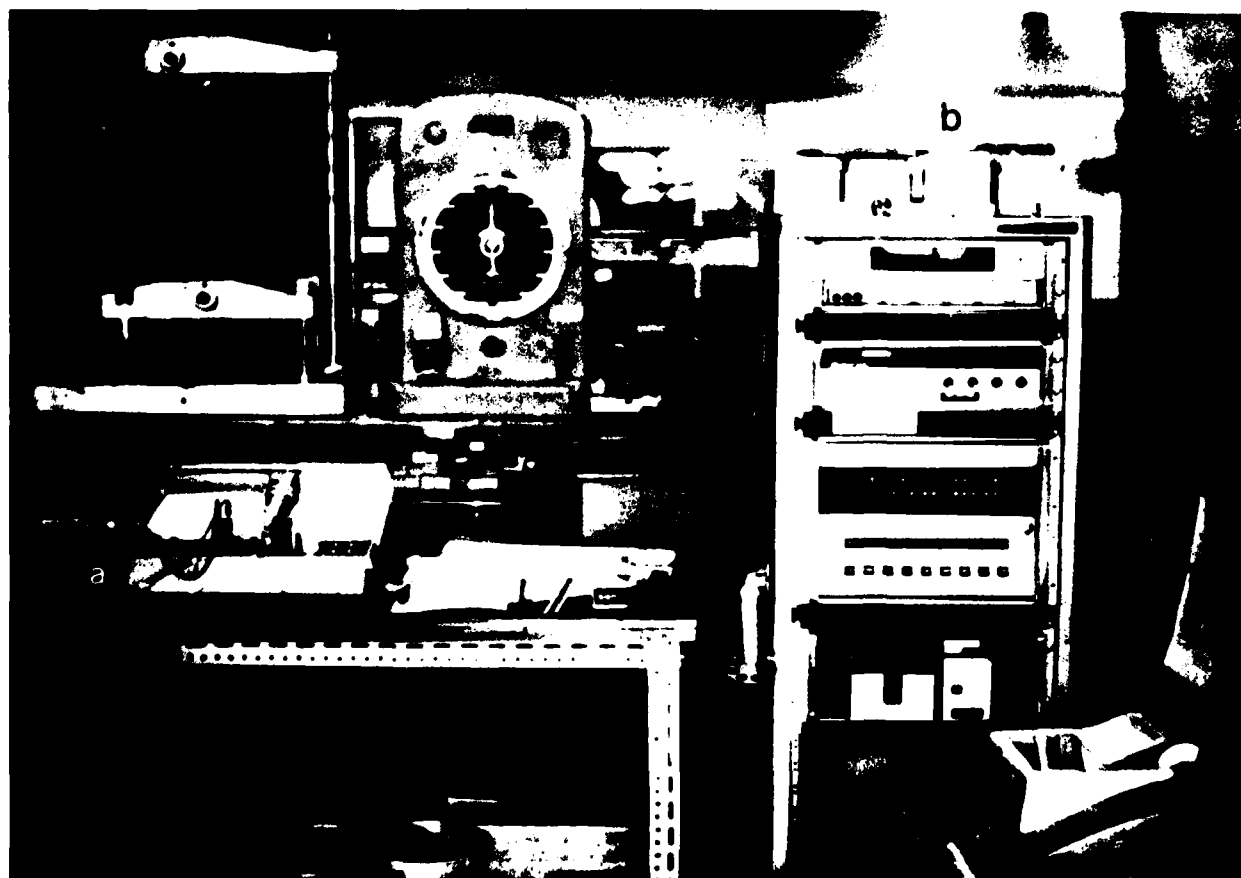


Figure 6.—Automatic data recording was accomplished with (a) an X-Y plotter, (b) an online computer, and (c) a teletype machine with paper tape punch.

Data Processing

Each test in groups one to four was processed to yield a plot of moment versus curvature. From these plots four properties were extracted: stiffness, strength, ductility, and knee-shape. To do this, the Ramberg-Osgood function was fitted to the plots of M versus $\frac{c}{R}$:

$$\frac{c}{R} = \frac{Mc}{EI} + K \left(\frac{Mc}{EI} \right)^n \quad (7)$$

where c = half depth = 2.75 inches, EI = flexural rigidity, pounds-inches²; and K and n are fitted parameters. To minimize rounding error in the curve fitting computations it is better to write equation (7) in the form

$$\frac{c}{R} = x + \exp \left[\ln(y_u) + n \ln \left(\frac{x}{x_u} \right) \right] \quad (8)$$

where $x \equiv \frac{Mc}{EI}$, $x_u \equiv x$ at ultimate load, and $y_u \equiv \left(\frac{c}{R} - \frac{Mc}{EI} \right)$ at ultimate load. This reduces to the Ramberg-Osgood form (eq. (7)) if $K \equiv \frac{y_u}{x_u^n}$. K is not a convenient parameter since it

can easily become so large that it overflows the floating point accumulator of a digital computer. Fitting the function given by equation (8), the four desired properties can easily be identified with the following fitted parameters:

EI = stiffness, x_u = strength, y_u = ductility, and n = knee-shape.

Figure 7 shows a typical fitted curve and the geometric meaning of the four properties. Hereafter this moment-curvature characteristic will be referred to as the "property" curve since it is uniquely specified by the four relevant properties. Note that the tail of the test record beyond maximum load is ignored in fitting the Ramberg-Osgood function, because this is a test machine artifact and not relevant to the dead-load conditions for which members are designed.

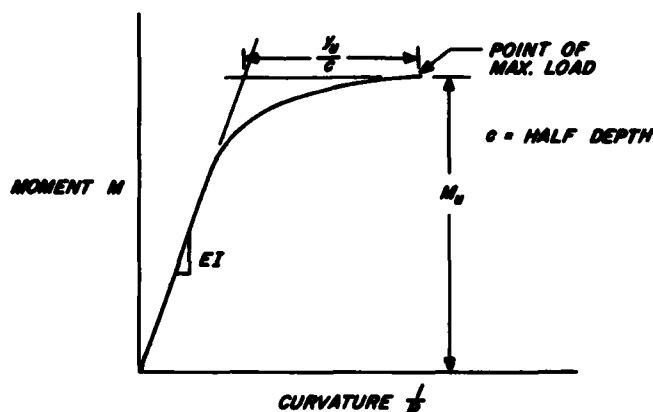


Figure 7.—Typical plot of moment versus curvature, from which four element properties can be derived: stiffness EI , strength M_u , ductility y_u , and shape n . Larger n implies a sharper knee.

Minor Tests

After testing the strength specimens to destruction, small coupons approximately 1.5 by 1.5 by 5.5 inches were cut from each and used to measure specific gravity and moisture content. The results are summarized for each group in table 2 which shows means followed by coefficient of variation in

parentheses. It is seen that these properties did not vary appreciably between groups. Therefore no adjustments were made to the data to correct for these variations.

Results of Experiments

Short Specimens—Groups One to Four

The results of the short member tests were four properties of each specimen obtained by fitting a Ramberg-Osgood function as described under Data Processing. There were four groups of specimens corresponding to four eccentricities as shown in table 1. Within each group a normal probability curve was fitted to each of the four properties, stiffness EI , strength x_u , ductility y_u , and knee-shape n , and to the quality index, E_r . In some cases it was found that the logarithm of the property was more nearly normal than the property itself. Specifically, the following properties were fitted with a multivariate normal probability curve:

Stiffness— EI , Strength— $\ln M_u$, Ductility— $\ln y_u$, Knee-shape— $\ln n$, Quality— E_r , where M_u is the moment at maximum load and E_r is the E-rating index of quality obtained from a preliminary nondestructive test as described under Specimen Preparation. The results of these curve fittings are summarized in table 3 which gives the means and the matrix of covariance for groups one to four.

Since the covariance matrix is diagonally symmetric, it contains only 15 independent elements. These plus the 5 means form 20 independent statistics for each group. These shall be denoted as S_1 through S_{20} defined such that

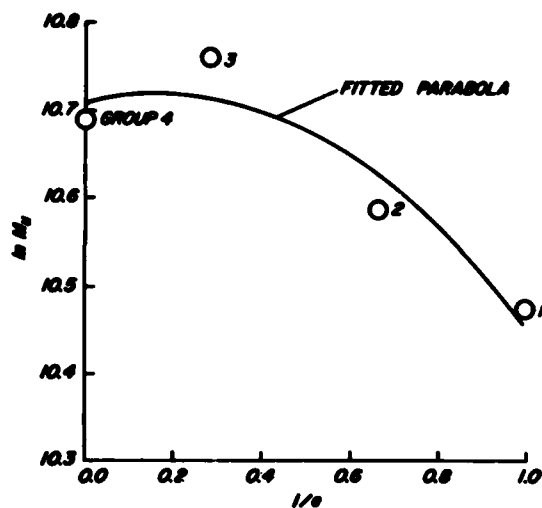
$$\text{Mean of } \begin{bmatrix} EI \\ \ln(M_u) \\ \ln(y_u) \\ \ln(n) \\ E_r \end{bmatrix} = \begin{bmatrix} S_1 \\ S_2 \\ S_3 \\ S_4 \\ S_5 \end{bmatrix}$$

$$\text{Covariance matrix} = \begin{bmatrix} S_6 & S_7 & S_8 & S_9 & S_{10} \\ \bullet & S_{11} & S_{12} & S_{13} & S_{14} \\ \bullet & \bullet & S_{15} & S_{16} & S_{17} \\ \bullet & \bullet & \bullet & S_{18} & S_{19} \\ \bullet & \bullet & \bullet & \bullet & S_{20} \end{bmatrix}$$

(diagonally symmetric)

For example, S_6 is the covariance of EI and $\ln y_u$. Together, the 20 statistics for any one group uniquely specify a multivariate (specifically five-variate) normal distribution that characterizes that group.

It should be noted that the characteristic multivariate distribution depends on e , the eccentricity of the group. All 20 statistics (with the exception of S_1 and S_{20} , the mean and variance of E_r) are functions of eccentricity e . Figure 8 shows, as an example, how the mean of the strength parameter $\ln M_u$ varies with eccentricity. For convenience in treating group four (pure bending, $e = \infty$) the statistics are plotted against the reciprocal of e and group four is at the origin. Note that the expected results were obtained: pure bending does not have the highest moment capacity. It is interesting to plot this in a plane of moment versus axial force. Figure 9 shows such a plot. It is seen that the addition of a small amount of axial compression does indeed increase the moment capacity for members tested over a short gage length.



M 148 611

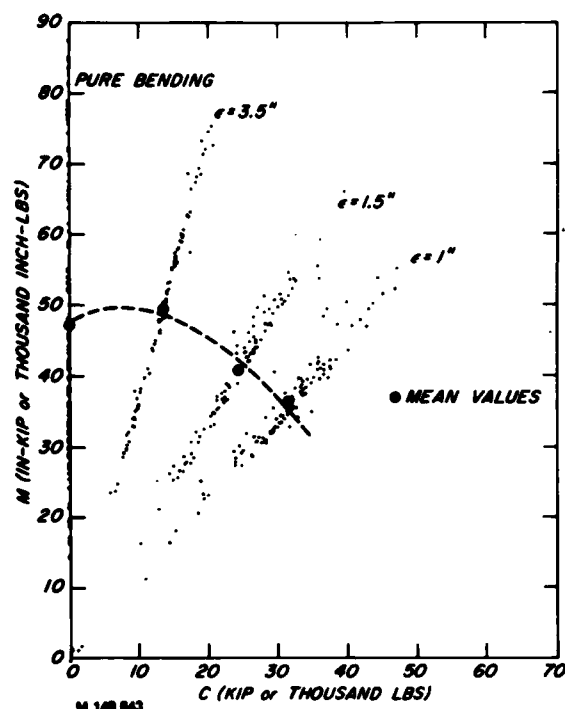
Figure 8.—Variation of input distribution with eccentricity. The mean of $\ln M_u$ is shown, along with a fitted parabola.

Long Specimens—Group Five

It is tempting at this point to simply use the data of groups one to four as a basis for design of members under combined bending and compression. However, the effect of length (including the possibility of plastic buckling) is critical and is not contained in figure 9. Group 5 shows this. It had the same eccentricity as group one but different length and, as table 2 shows, its mean ultimate load was only about half of that of group one. The E_r distributions of groups five and one are not quite as closely matched as those of groups one to four but are still very close. This comparison clearly shows that there is a profound length effect. It is due to plastic instability in the presence of material asymmetries around defects and variable stiffness along the length. Such an effect is difficult to analyze mathematically in closed form. A nonlinear, numerical analysis is done in the next section, where the E_r variation along the length of the members in group five is used as an input to a non-standard finite element simulation of the group five specimens.

Monte Carlo Simulation of Length Effect

Group five specimens were simulated with the special finite element analysis given in the appendix. In that analysis the nonlinear Ramberg-Osgood function given in equation (7) is used to represent the relationship between moment and curvature. This equation is exactly solved by iteration for each given set of four Ramberg-Osgood properties: EI , x_u , y_u , and n . These properties are assumed to be piecewise constant functions of x with five "pieces" or "finite elements" covering the range of x . Deflections and slopes are matched at the nodes between elements. This is far more exact than a standard finite element approach which would approximate deflection shapes over each element and would account for geometric nonlinearity in an approximate manner via the so-called stability matrix. Since the number of elements could not be made large here, it was decided to use a more exact non-standard finite element method. Five 19-inch elements



M 148 643

Figure 9.—Results of short member tests: failure moment versus failure load (both measured at point of maximum load) for groups one to four (KIPS = thousand lbs).

add up to a 95-inch-long member — essentially 8 feet. The results of the short member tests, which had a gage length of 18 inches, were used in a five-element model to simulate the behavior of the group five specimens. The error of using data obtained over 18 inches in a 19-inch element is negligible.

Input Parameters

In the Monte Carlo technique, input parameters are randomly selected from a known distribution and a test is simulated. This is repeated many times until enough output strength values have been generated to give an idea of the output distribution.

In this case the input was of two kinds: (1) the distribution of element properties and (2) a quality description of the long member to be simulated. Input (1) consisted of a five-variate normal distribution in the variable EI , $\ln(M_u)$, $\ln(y_u)$, $\ln(n)$, and E_r . This was specified by a five-vector of means and a five by five symmetric covariance matrix, that is, by 20 independent statistics. See equations (9) and (10). With the exception of E_r and its variance, each of these statistics is a function of the eccentricity of the element as can be seen by examining table 3 and figure 8. Hence each was specified by the three coefficients of a parabola

$$S_i = a_i \left(\frac{1}{e}\right)^2 + b_i \left(\frac{1}{e}\right) + c_i \quad (11)$$

Here a_i , b_i , and c_i are the fitted coefficients, S_i is a statistic fitted by least squares to the data in table 3, and e is the eccentricity. These coefficients are shown in table 4. The other input (2) consisted of the E_r values of the five elements of the long member to be simulated. These had been obtained nondestructively for the specimens in group five before testing them in eccentric axial compression.

Random Selection of Elements

The Monte Carlo technique proceeded as follows:

For each element with a given measured value of E_r ,

1. Generate four independent random normal variates with zero mean and unit variance:

$$z = \begin{bmatrix} z_1 \\ z_2 \\ z_3 \\ z_4 \end{bmatrix} \quad (12)$$

$$\begin{bmatrix} EI \\ \ln(M_u) \\ \ln(y_u) \\ \ln(n) \\ E_r \end{bmatrix} = \text{Normal with mean } \mu \text{ and covariance } \Sigma$$

where

$$\mu = \begin{bmatrix} S_1 \\ S_2 \\ S_3 \\ S_4 \\ S_5 \end{bmatrix} \quad (13)$$

This vector will be used in step 4. It identifies the randomly-chosen element.

2. Using the current eccentricity e of the element, calculate the parameters S_1 through S_{20} of the element property distribution at this eccentricity:

Table 3.—Summary of property statistics

Statistic	Group			
	1	2	3	4
MEANS (see eq. (9))				
$S_1 = \text{mean}(EI)$	0.444761 + 08	0.400781 + 08	0.391585 + 08	0.448324 + 08
$S_2 = \text{mean}(\ln M_u)$.104730 + 02	.105860 + 02	.107590 + 02	.106890 + 02
$S_3 = \text{mean}(\ln y_u)$	-.687770 + 01	-.672110 + 01	-.688740 + 01	-.787720 + 01
$S_4 = \text{mean}(\ln n)$.205100 + 01	.219090 + 01	.209800 + 01	.165650 + 01
$S_5 = \text{mean}(E_r)$.104183 + 07	.104678 + 07	.102889 + 07	.104045 + 07
COVARIANCES (see eq. (10))				
$S_6 = \text{var}(EI)$.133746 + 15	.106474 + 15	.938794 + 14	.107557 + 15
$S_7 = \text{cov}(EI, \ln M_u)$.138715 + 07	.153167 + 07	.227157 + 07	.326864 + 07
$S_8 = \text{cov}(EI, \ln y_u)$	-.405308 + 07	-.179065 + 07	-.176640 + 07	.378817 + 06
$S_9 = \text{cov}(EI, \ln n)$.115347 + 07	.217908 + 07	.256852 + 07	.191873 + 07
$S_{10} = \text{cov}(EI, E_r)$.106694 + 13	.126682 + 13	.153258 + 13	.141881 + 13
$S_{11} = \text{var}(\ln M_u)$	0.632824 - 01	0.578820 - 01	0.116250 + 00	0.192532 + 00
$S_{12} = \text{cov}(\ln M_u, \ln y_u)$.473633 - 01	.309349 - 02	.291294 - 01	.772557 - 01
$S_{13} = \text{cov}(\ln M_u, \ln n)$.243918 - 01	.456674 - 01	.116520 + 00	.885921 - 01
$S_{14} = \text{cov}(\ln M_u, E_r)$.254907 + 05	.274862 + 05	.470426 + 05	.444307 + 05
$S_{15} = \text{var}(\ln y_u)$.685311 + 00	.451765 + 00	.106489 + 01	.995538 + 00
$S_{16} = \text{cov}(\ln y_u, \ln n)$.420844 - 01	-.145156 - 01	.153682 + 00	.703405 - 01
$S_{17} = \text{cov}(\ln y_u, E_r)$	-.298365 + 05	-.225922 + 05	-.351988 + 05	.915227 + 04
$S_{18} = \text{var}(\ln n)$.217163 + 00	.328039 + 00	.547928 + 00	.386828 + 00
$S_{19} = \text{cov}(\ln n, E_r)$.957648 + 04	.174911 + 05	.558619 + 05	.337252 + 05
$S_{20} = \text{var}(E_r)$.352101 + 11	.314806 + 11	.469594 + 11	.268380 + 11

and

$$\Sigma = \begin{bmatrix} S_6 & S_7 & S_8 & S_9 & S_{10} \\ S_7 & S_{11} & S_{12} & S_{13} & S_{14} \\ S_8 & S_{12} & S_{15} & S_{16} & S_{17} \\ S_9 & S_{13} & S_{16} & S_{18} & S_{19} \\ S_{10} & S_{14} & S_{17} & S_{19} & S_{20} \end{bmatrix} \quad (14)$$

where $S_i, i=1,20$ are given by equation (11) as functions of e . (Note that S_1 and S_{20} are independent of e , so the given E_T is always constant.)

3. With this μ and Σ and the given E_T , calculate a conditional four-variate property distribution:

$$\begin{bmatrix} EI \\ \ln(M_U) \\ \ln(y_U) \\ \ln(n) \end{bmatrix} = \text{Normal with mean } \hat{\mu} \text{ and covariance } \hat{\Sigma}$$

where

$$\hat{\mu} = \begin{bmatrix} S_1 \\ S_2 \\ S_3 \\ S_4 \end{bmatrix} + \frac{E_T - S_5}{S_{20}} \begin{bmatrix} S_{10} \\ S_{14} \\ S_{17} \\ S_{19} \end{bmatrix} \quad (15)$$

and

$$\hat{\Sigma} = \begin{bmatrix} S_6 & S_7 & S_8 & S_9 \\ S_7 & S_{11} & S_{12} & S_{13} \\ S_8 & S_{12} & S_{15} & S_{16} \\ S_9 & S_{13} & S_{16} & S_{17} \end{bmatrix} - \frac{1}{S_{20}} \begin{bmatrix} S_{10} & S_{10}S_{14} & S_{10}S_{17} & S_{10}S_{19} \\ S_{14}S_{10} & S_{14}^2 & S_{14}S_{17} & S_{14}S_{19} \\ S_{17}S_{10} & S_{17}S_{14} & S_{17}^2 & S_{17}S_{19} \\ S_{19}S_{10} & S_{19}S_{14} & S_{19}S_{17} & S_{19}^2 \end{bmatrix} \quad (16)$$

4. Calculate the four element properties

$$\begin{bmatrix} EI \\ \ln(M_U) \\ \ln(y_U) \\ \ln(n) \end{bmatrix} = (\hat{\Sigma})^{\frac{1}{2}} \cdot Z + \hat{\mu}$$

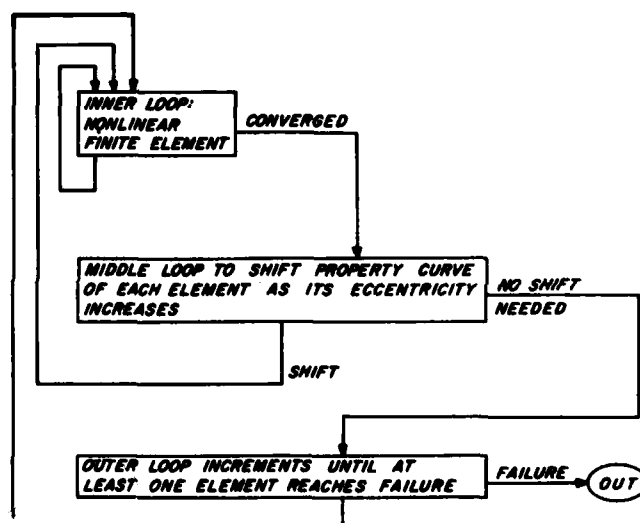
From these four values the property curve, equation (8), of the element can be determined.

Element Identity

As load increases the eccentricity of any given element increases in response to the increasing deflections of the member. And since it was found that characteristic element behavior is different at different eccentricities it was decided to let the characteristic property distribution of the element evolve as a function of $\frac{1}{e}$, where e is the current eccentricity of that element. Thus, element properties are not constant and cannot be said to identify the element. However, the z vector can be used to identify the element, since it specifies the number of standard deviations away from the mean that the element lies within its distribution. If this is held constant, the element keeps its rank order relative to other elements in the distribution. This is like assuming that the rank order of the short specimens in any group would have been the same if they had been tested at any other eccentricity. (This assumption is a useful expedient, but it may not be strictly true, since the relative severity of defects may be influenced to some extent by the eccentricity of the load.)

Table 4.—Coefficients of fitted parabolas (see eq. (11))

i	a _i	b _i	c _i
1	0.233530 + 08	-0.232150 + 08	0.445578 + 08
2	-.384481 + 00	.135828 + 00	.107071 + 02
3	-.274490 + 01	.365608 + 01	-.782813 + 01
4	-.139041 + 01	.175730 + 01	.167184 + 01
5	0.0	0.0	.103719 + 07
6	.922241 + 14	-.646011 + 14	.106760 + 15
7	.220646 + 07	-.408230 + 07	.326550 + 07
8	-.131435 + 06	-.374509 + 07	.702772 + 05
9	-.380925 + 07	.298817 + 07	.194974 + 07
10	-.666018 + 12	.266089 + 12	.144551 + 13
11	.207180 + 00	-.338225 + 00	.193529 + 00
12	.222322 + 00	-.255763 + 00	.792267 - 01
13	-.908562 - 01	.177533 - 01	.975369 - 01
14	-.605811 + 04	-.170433 + 05	.467426 + 05
15	.522511 + 00	-.994989 + 00	.108568 + 01
16	-.261666 - 01	-.548651 - 01	.996603 - 01
17	.852618 + 05	-.114556 + 06	.376651 + 04
18	-.583959 + 00	.358354 + 00	.417622 + 00
19	-.613884 + 05	.271180 + 05	.393484 + 05
20	0.0	0.0	.304231 + 11



M 140 873

Figure 10.—Block diagram of computing method.

Computing Method

Figure 10 shows a block diagram of the computing method. The inner loop is necessitated by the nonlinearity of the moment-curvature relationships of the elements. The moment-curvature relationship, or "property curve," is represented here as a Ramberg-Osgood function as discussed under Data Processing. As the deflections increase, the property curves must shift in response to the increasing eccentricities of the elements. This necessitates a middle loop of iterations until the deflections of the nonlinear finite element solution are congruent with the eccentricities used to derive the properties of each element. Finally, there is an outer loop in which the load is gradually incremented until at least one element reaches failure. If these increments are not too large, convergence of the inner loops will be very rapid. A complete flow diagram of the subprogram SIMTST used to simulate an eccentrically loaded member is shown in figure 11. Computing time to simulate one destructive load test of a five-element member was about 4 seconds on a Univac 1110 computer.

Results of Monte Carlo Simulations

Verification of the Model

Figure 12 shows a comparison of model and experimental results. Group five consisted of a small sample of just 29 members of 8-foot gage length under 1-inch eccentric axial load. This group was included in the study in order to

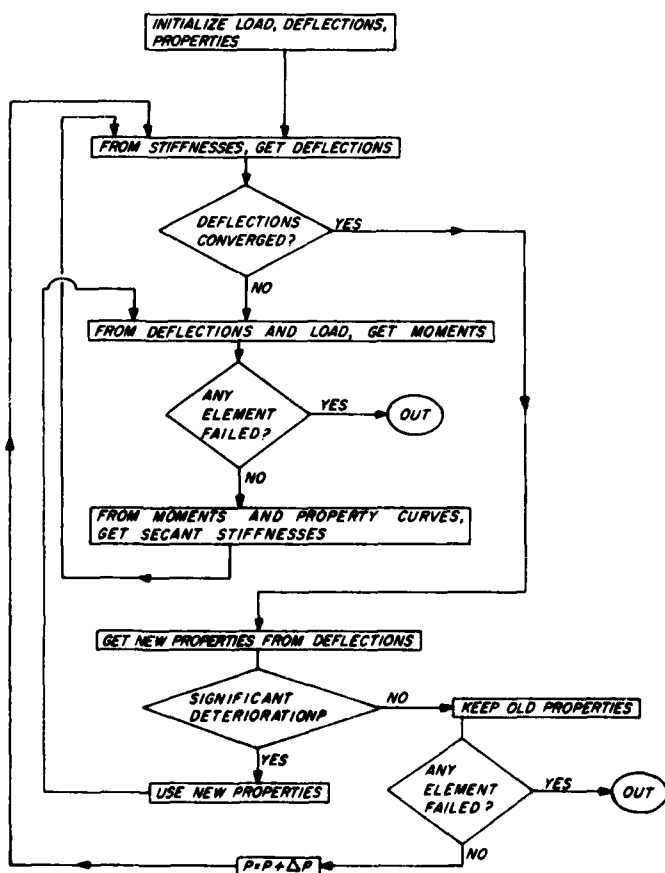


Figure 11.—Flow diagram for program SIMTST, the finite element simulation of a long member test.

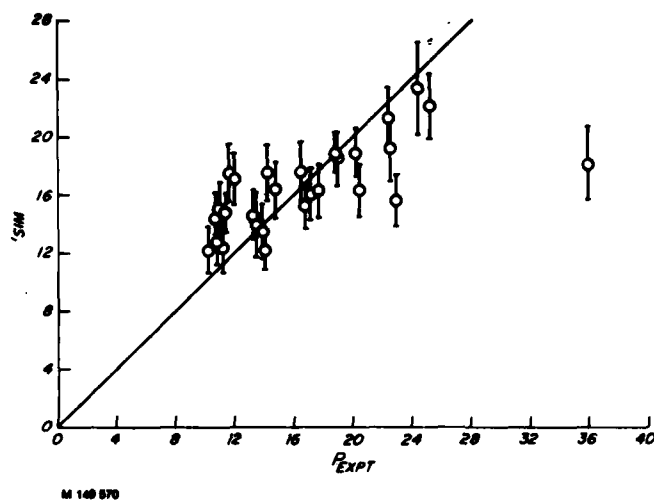


Figure 12.—Simulated failure load of 8-foot-long members versus experimental failure loads of group five.

roughly verify the computer finite element model. Each test member had been E-rated at five locations within the gage length, and the computer used these ratings as input specifications for a five-element simulation. Each member was simulated 30 times with element properties chosen randomly from conditional distributions, given the input E-ratings. The simulations are shown in figure 12 as vertical lines representing the mean plus or minus one standard deviation. The 45° lines show where the data should fall for perfect verification. It is seen that the mean of group five is accurately reproduced but that the variance is underestimated. That is, the trend of the data is not a 45° line as it should be. This suggests that there may be a better index of quality than the edgewise E-rating. Perhaps flatwise E would prove to be more sensitive. The correlation coefficient between E_r and $\ln M_u$ was only

$$\text{correlation coefficient} = \begin{bmatrix} 0.54 \\ 0.64 \\ 0.64 \\ 0.60 \end{bmatrix} \text{ for group } \begin{bmatrix} 1 \\ 2 \\ 3 \\ 4 \end{bmatrix} \quad (18)$$

in this study, which is not very great. The correlation between the E_r of the center element and the ultimate load for group five was also small, namely 0.68. But the fact remains that the correlation between strength and nondestructive quality indices is never very great. This is the essential problem of lumber grading translated here into element grading. Nevertheless it may be possible to force the computer model to do better in the aggregate even though it remains a somewhat poor predictor for individual members. This is worthy of further study.

The Effect of Length

The effect of length has been discussed briefly above in the comparison of experimental results for groups one and five. A more thorough investigation of the effect of length can be made with the use of the computer model. Figure 13 shows how the 29 specimens in group five would have behaved if they had been tested at other eccentricities or in pure bending. Each specimen is represented by the average of 30 simulations and mean and standard deviation of the sample of 29 is

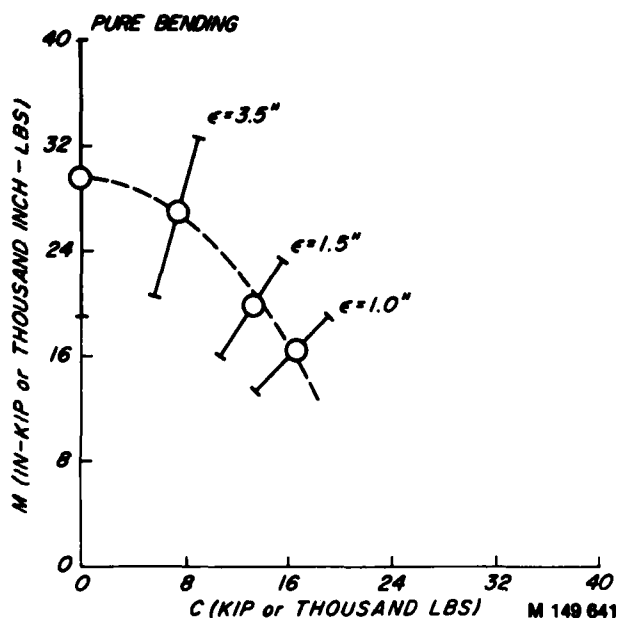


Figure 13.—Computer simulations of 8-foot-long members under eccentric axial load.

plotted in the figure. Deflections due to load are ignored in plotting moment versus axial load, that is:

$$M = Pe \quad (19)$$

is used rather than

$$M = Pd \quad (20)$$

even though the deflection δ might be quite large. This was done for the sake of facilitating application to design. The design engineer knows the eccentricity e but cannot accurately estimate the lateral deflection δ especially when plastic buckling is a possibility.

It is seen in figure 13 that the mean moment capacity does not improve with the addition of a small amount of axial compressive force as was found for groups one to four. However, the low tail of the distribution *does* still exhibit this effect, though it is far less pronounced than it was for the short specimens (compare fig. 9). Before this effect can be counted upon in design, other loadings and different species and sizes should be investigated. Also, the behavior of the computer model in the low tail may not be reliable since the model is known to underestimate variability. Of course, for very long members, failure by buckling will appear at low compressive loads. Even at 8 feet the influence of some inelastic buckling is already evident, as can be seen by comparing figures 9 and 13. In this comparison it is important that the grade of the small population in group five should resemble the grade of the populations in groups one to four. Figure 14 shows a comparison of the E_r distribution of group five to the common E_r distribution of groups one to four. It is seen that the resemblance is quite close although no special attempt was made to select group five members for this match. Also, the comparison of figures 9 and 13 is a comparison of simulated members with real test specimens, so modeling error is present. The model underestimates variability. Thus the comparison should be restricted to the means. Nevertheless, the comparison strongly indicates that the effect of length is a profound one. Three things contribute to this: inelastic

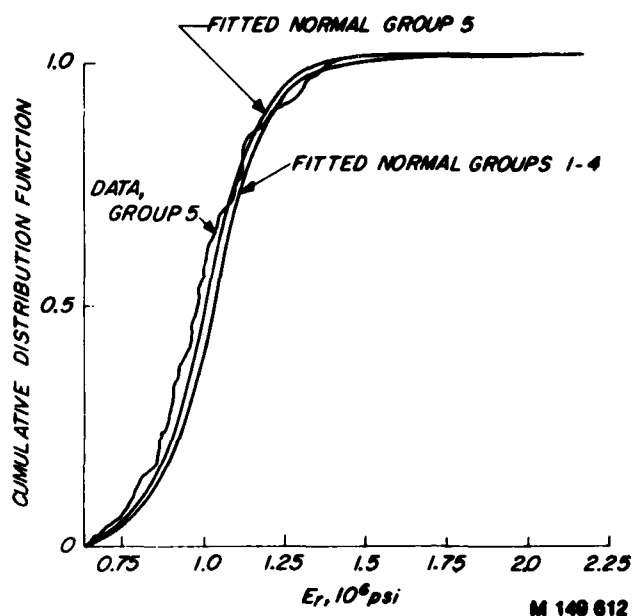


Figure 14.—Comparisons of E_r distributions of group five and groups one to four.

buckling, size effect, and the interaction of bending and compression failure.

Summary

The interaction of bending and compression strengths of western hemlock 2 by 6 lumber was investigated. Over 400 short specimens (with gage length = 18 in.) were tested in four groups with different ratios of moment and compression. Some interaction was found that decreases with increasing length, as shown by the results of a finite element simulation also reported here. This finite element model was able to reproduce mean results of a small sample of 8-foot-long specimens but did not show as large a variation as the experimental data. The model could be greatly improved if a better nondestructive index of quality could be found which correlated better with strength than the edgewise bending stiffness used here. Perhaps a combination of two indices should be used.

Data should be obtained for other sizes and species. The results could be used by researchers studying the reliability of wood walls and roof-truss systems. The data presented here are sufficient to show that a simple linear interaction failure criterion is conservative—the degree of conservatism being greater for shorter members.

Literature Cited

1. Bohannon, B.
1974. Time-dependent characteristics of pre-stressed beams. USDA For. Serv. Res. Pap. FPL 226, For. Prod. Lab., Madison, Wis.
2. Hildebrand, F. B.
1952. Difference equations. Methods of Applied Mathematics. Prentice-Hall, Inc., Englewood Cliffs, N. J.

Appendix: Finite Element Analysis

Combined Bending and Compression

Consider a member of length L under eccentric axial load and divide the member into m equal elements of length h as shown in figure A1.

$$L = mh \quad (A1)$$

Isolate the n th element. From elementary beam theory the moment-curvature relationship is

$$(EI)_n y_n'' = -Py_n \quad (A2)$$

where y_n = lateral deflection in the range $(n-1)h \leq x \leq nh$ measured from the line of action of P and primes denote differentiation with respect to x . Let the nodal displacements be q_n :

$$y = q_n, \text{ at } x = nh, \quad n = 0, m \quad (A3)$$

The solution of differential equation (A2) which satisfies boundary conditions (eq. (A3)) is

$$y_n = \left[\frac{q_n \cos(n-1)\lambda_n h - q_{n-1} \cos(n\lambda_n h)}{\sin \lambda_n h} \right] \sin \lambda_n x + \left[\frac{-q_n \sin(n-1)\lambda_n h + q_{n-1} \sin(n\lambda_n h)}{\sin \lambda_n h} \right] \cos \lambda_n x \quad (A4)$$

where

$$\lambda_n \equiv \sqrt{\frac{P}{(EI)_n}}$$

Match slopes at n th node:

$$y_n' = y_{n+1}' = 0 \text{ at } x = nh \quad (A6)$$

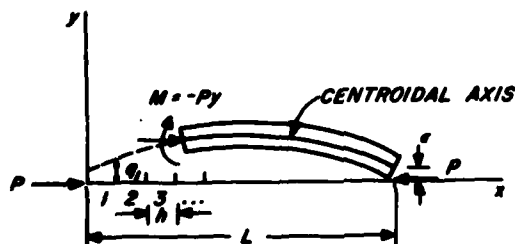
Substituting equation (A4) into (A6) and using some trigonometric identities this becomes

$$\left\{ -\frac{\lambda_n}{\sin \lambda_n h} \right\} q_{n-1} + \left\{ \frac{\lambda_n \cos \lambda_n h}{\sin \lambda_n h} + \frac{\lambda_{n+1} \cos \lambda_{n+1} h}{\sin \lambda_{n+1} h} \right\} q_n + \left\{ -\frac{\lambda_{n+1}}{\sin \lambda_{n+1} h} \right\} q_{n+1} = 0 \quad (A7)$$

Equation (A7) yields a banded matrix of $m-1$ equations for $m+1$ unknown q_0 to q_m . But, of course, two of the nodal displacements are given:

$$q_0 = q_m = \epsilon \quad (A8)$$

where ϵ is the given eccentricity. Thus all nodal displacements can be obtained by solving an $(m-1)$ th order linear system if the λ_n are given. For small loads, the $(EI)_n$ are constants independent of P . For larger P one must obtain $(EI)_n$ from the secant to the point on the property curve corresponding to the load. To find this point requires some iteration, since the deflections depend on the $(EI)_n$, the $(EI)_n$ depend on the moments, and the moments depend on the deflections. A few iterations around this loop will quickly converge, however, especially if one starts



M 149 800

Figure A1.—Free-body diagram of member under eccentric axial load. Centroidal deflection y is measured from line of action of load P .

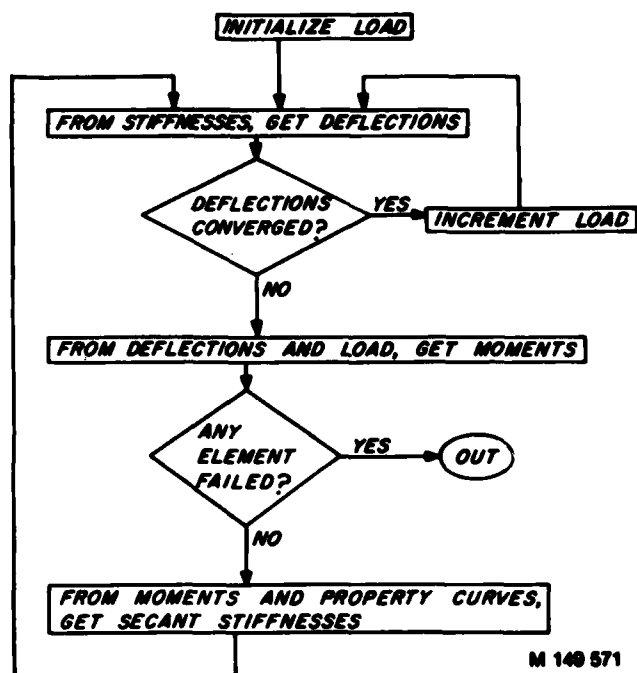
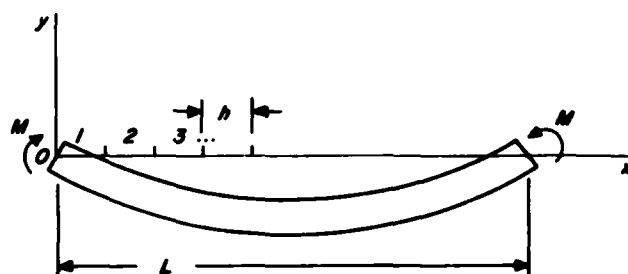


Figure A2.—Iteration loop used in finite element simulation program.



M 140 508

Figure A3.—Free-body diagram of member under pure bending.

with a good initial guess. Hence for large loads one must begin with a load small enough to ensure linear behavior and increase by small increments, iterating to convergence after each increment, and using the solution from the last load as the initial guess for the $(EI)_n$ after each increment. This procedure continues until one of the elements reaches its failing load. Figure A2 shows the iteration loop.

This method is capable of accurately modeling the phenomenon of plastic buckling when all elements are sufficiently ductile. In that case the deflections grow rapidly just before failure.

Pure Bending

In the case of pure bending the finite element analysis is greatly simplified by the absence of any buckling phenomenon. Consider a member of length L under pure bending as shown in figure A3. Again cut the member into m elements of length h so that

$$L = mh \quad (A9)$$

Isolate the n th element. The moment-curvature relationship is

$$(EI)_n y''_n = M \quad (A10)$$

where y_n = lateral deflection in the range $(n-1)h \leq x \leq nh$. Let nodal displacements be q_n :

$$y = q_n \text{ at } x = nh, n = 0, m \quad (A11)$$

The solution of equation (A10) satisfying conditions (A11) is

$$y_n = \mu_n \left(\frac{x^2}{2} \right) - \mu_n h \left(n - \frac{1}{2} \right) x + \mu_n \left(\frac{h^2}{2} \right) n(n-1) + q_n \left(\frac{x}{h} \right) - (n-1)q_n - q_{n-1} \left(\frac{x}{h} \right) + nq_{n-1} \quad (A12)$$

where

$$\mu_n = \frac{M}{(EI)_n} \quad (A13)$$

Match slopes at n th node:

$$y'_n = y'_{n+1} = 0, x = nh \quad (A14)$$

Substituting (A12) into (A14) and simplifying yields

$$q_{n-1} - 2q_n + q_{n+1} = \frac{h^2}{2}(\mu_n + \mu_{n+1}) \quad (A15)$$

This is a finite difference equation whose solution can be obtained in closed form. The homogeneous solution is

$$q_n = \alpha + \beta n \quad (A16)$$

where α and β are arbitrary constants. Now let α and β be functions of n :

$$q_n = \alpha_n + \beta_n n \quad (A17)$$

and use the method of variation of parameters (2) to find

$$\alpha_n = -\sum_0^{n-1} (i+1) \frac{h^2}{2} (\mu_i + \mu_{i+1}) + A \quad (A18)$$

$$\beta_n = \sum_0^{n-1} \frac{h}{2} (\mu_i + \mu_{i+1}) + B \quad (A19)$$

where A and B are constants analogous to integration constants. They are determined by the conditions

$$q_0 = 0 \quad (A20)$$

and

$$q_m = 0 \quad (A21)$$

from which

$$A = 0 \quad (A22)$$

and

$$B = -\frac{h^2}{2m} \sum_1^m (m-i) (\mu_i + \mu_{i+1}) \quad (A23)$$

Thus after simplification, we find

$$q_n = -\frac{h^2}{2m} \left\{ (m-n) \sum_1^m (2i-1) \mu_i + n \sum_{n+1}^m (2m-2i+1) \mu_i \right\} \quad (A24)$$

From the nodal displacements, the deflection at the center of the n th element is calculated to be

$$\delta_n = \frac{q_{n-1} + q_n}{2} + \left(\frac{h^2}{2}\right) \mu_n \quad (A25)$$

The computer algorithm proceeds as follows:

1. The strength of the member is the strength of the weakest element.
2. At failing load, the center deflection of the member is computed from (A25), using (A24) and (A13).

U.S. Forest Products Laboratory

Strength of Lumber Under Combined Bending
and Compression, by John J. Zahn, Res. Pap. FPL
391, FPL, For. Serv., USDA. 13 p. Madison, Wis.

Extensive tests of western 2 by 6's under
eccentric axial load support the conjecture that
adding a small compressive force increases bending
strength. Length effect was tested on short test
members by simulating long members with a finite
element computer program. A small sample of
long members was tested for verification of the
model which accurately reproduces the mean but
underestimates the variance. Further work on the
model will be applicable to column and wood truss
design.

END

FILMED

1-83

DTIC